Distributed Generation Inverter: New control Strategies to Supply Local Load with Standard Voltage under Distorted Grid Voltage

MAHDI SHAHPARASTI[1]

[1] *Department of Electrical Engineering, Islamic Azad University, East Tehran Branch, Tehran, Iran*
[*] *Corresponding author: mahdi.shahparasti@upc.edu*

Manuscript received 12 February, 2019;Revised 26 April, 2019, accepted 30 May, 2019. Paper no. JEMT-1902-1154.

In this paper, two control strategies are proposed for distributed generation inverter (DGI) to control 1) active power exchange with the grid, 2) load voltage and 3) grid current. The main goal in these strategies is supplying local load with a standard sinusoidal voltage in the presence of grid voltage distortions and load current nonlinearity. In conventional DGIs, the load is directly and without intermediate impedance connected to the grid; thus, the possibility of load feeding with appropriate voltage quality is hindered in the grid connected mode. In order to overcome this deficiency, DGI with an LC-L filter topology and two control strategies are presented in this paper to supply the local load with standard voltage and to exchang power with the grid, simultaneously. In the first control strategy, the local load is supplied with pure sinusoidal voltage and grid current quality is not important. In the second control strategy, load voltage waveform and grid current waveform are controlled by adding appropriate harmonics to load voltage. For the implementation of the mentioned control strategies, a cascade power-voltage-current control structure has been proposed. A new controller has been introduced in the stationary reference frame for the voltage loop which gives the opportunity for compensation and tracking of harmonics without the need for complex and vast calculations. Test results under nonlinear load and non-ideal grid conditions validate that the proposed method can supply the local load with a standard voltage, inject power to the grid, and also control the grid current.

keywords: *Distributed generation inverter (DGI), DC/AC energy conversion, Inverter control in standalone mode, Inverter control in grid-connected mode, harmonic compensation.*

http://dx.doi.org/10.22109/jemt.2019.171597.1154

NOMENCLATURE

C_f	capacitor of LC filter
$G_i(s)$	current controller
$G_v(s)$	voltage controller
g_i	inverter gain
Hf	harmonic factor
i	inverter current
i_g	current of the grid
GT	Gas turbine
i_{load}	load current
i_{gh}	h^{th} harmonic of the grid current
k_{il}	integral gain
k_{pl}	proportional gain
L	interface inductor
L_f	inductor of LC filter
P^*	active power reference
R	equivalent resistance of output load
r	equivalent resistance of interface inductor
THD	total Harmonic Distortion
V	voltage of the load

Table 1. IEEE1547 and IEC1727 requirements for harmonics of load voltage and grid current.

Individual Harmonic order	Percent (%)
$h < 11$	4.0
$11h < 17$	2.0
$17h < 23$	1.5
$23h < 35$	0.6
$35h$	0.3
THD	5.0

V^* voltage reference

V_g voltage of the grid

V_i output voltage of inverter bridge

V_h h^{th} harmonic of the load voltage

V_{gh} h^{th} harmonic of the grid voltage

ω grid frequency

δ phase angle of voltage reference

1. INTRODUCTION

According to European H2030 roadmap, 37% of electrical energy has to be provided through the installation of distributed generators (DG) due to their economic and technical merits [1]. DGs include variable frequency AC sources (wind turbine and microturbine) and DC energy sources (PV and Fuelcells) [2,3] Generally, DGs are connected to the grid or the load consumer through DC/AC voltage source inverter (VSI) [4]. A distributed generation inverter (DGI) is used to transform the power of DGs to the Point of Common Coupling (PCC). DGI suppling local load has two operation modes: grid connected and standalone based on the grid status [5]. If the voltage and frequency of the grid are abnormal and nonstandard, the DGI is disconnected from the grid and the local load is fed in standalone mode with standard voltage. When the grid returns to the normal state, DGI once again connects to the grid. Up to now, various standards have been introduced to identify the criteria of load voltage quality and grid current quality according to the grid conditions [6]. Harmonic spectrum is the main criteria of grid current [7]. The requirements of IEEE 1547 standard for the maximum allowed harmonics in the load voltage and grid current are given in Table 1.

Fig. 1 shows two common hardware structures of DGI which have been presented in the studies for the connection of grid, load and VSI together. In Fig. 1 (a,b), there is a LC filter and a LCL filter between the VSI and the PCC, respectively. In grid connected mode, Fig. 1(b) has a better current profile in comparison to the structure in Fig. 1(a) , because LCL filters can eliminate the switching harmonics more efficiently. On the other hand, in the standalone mode more current is derived from the inverter to feed nonlinear loads compared to the LC filter. From control scheme point of view, DGI operates as a controlled current source while it is connected to the grid. The voltage quality of PCC directly affects the performance of the system response. The main aim of conventional control methods is to absorb sinusoidal current from VSI [7–10], so if the local load is nonlinear, thus the grid current is non- sinusoidal (equal to the difference between inverter current and load). DGI has to work as a voltage source with constant amplitude, fixed frequency and low THD in standalone mode [10]. Toggling between two working modes leads to applying a nonstandard voltage to the load and receiving an inrush current from the grid [12].

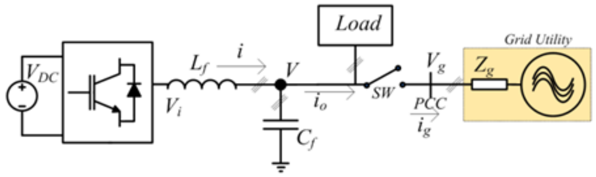

(a) DGI with LC filter

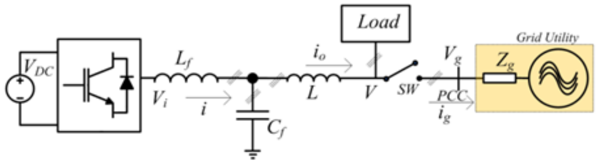

(b) DGI with LCL filter

Fig. 1. Single line diagram of common structures of DGI. (a) DGI with LC filter, (b) DGI with LCL filter

An H^∞ based current-voltage controller is presented in [13] to compensate load current harmonics, so the grid current is always sinusoidal. In [14] a parallel control system containing a load voltage loop and the current grid is proposed in which it is possible to obtain a seamless transformation between two working modes by changing the reference. In [12] and [15] the possibility of a seamless transform between working modes has been established by designing an appropriate phase locked loop (PLL). Droop control is proposed in [16–18] to control DGI, which has inherent seamless transform capability but its performance decline with grid impedance variations. Droop control is enhanced by addition of an extra control loop to system control, which is called the virtual output impedance in [19]. Virtual impedance has to be bigger than the sum of DGI output impedance and the grid impedance [20] . In [21], a controller is used based on the generic control framework of the synchronous power controller (SPC), which is able to control inverter power as well as compensate nonlinear current harmonics. [22,23] proposes a hierarchical control method for DGIs in the microgrid to compensate voltage distortions by injecting shunt current but there is no guarantee to supply the load with standard voltage. An active power filter based multi-level DGI has to be used only for compensating load harmonics in [24], which leads to improvement of PCC voltage waveform, but this could not compensate grid voltage harmonics. In total, existing control strategies mainly focus on either the quality of the grid current or the PCC voltage in the grid connected mode (load voltage in Fig.1), and improving both of them have not addressed yet.The DGI's criterion for connection and disconnection to and from the grid is the grid voltage amplitude and frequency. Based on the IEEE 1547 standard, in case of disturbances, the DGI can disconnect from the grid and feed load in standalone mode after a specific clearing time. In this standard, there is no talk about grid voltage harmonics and only the frequency and voltage amplitude are taken into account. In DGI conventional structures (Fig.

- Based on standard IEEE 1547 for the grid voltage amplitude between 88% and 110% of the nominal voltage, DGI has to remain connected to the grid.
- In standard IEEE 1547, there is no talk about grid voltage harmonic distortion. If the grid is distorted then the inverter has to remain connected to the grid.

This paper focuses on grid connected mode; the main goal is the improvement of the waveform quality of the grid current and the load voltage under non ideal grid voltages in the presence of nonlinear local loads. The main contribution of this paper is presenting new control strategies to supply the local load with standard voltage under aforesaid disturbances:

- LVC control strategy: supplying the local load with high quality voltage under aforesaid disturbances, and exchange active power with the grid, simultaneously.
- LVGCC control strategy: supplying the local load with standard voltage under aforesaid disturbances, to control current injected to the grid and exchange active power to the grid, simultaneously.

In Table 2, DGI capabilities with different control schemes are mentioned to highlight the contribution of this work. It is evident that the main object of this paper is to supply local load with standard voltage in grid-connected mode compared to other works.

This paper is organized as follows. Section 2 and 3 describe the LVC and LVGCC control strategies introduction and implementation, respectively. The hardware design of DGI is explained in Section 4. Section 5 provides frequency domain analysis, simulation results and comparative studies to verify the performance of the proposed control strategies. The conclusion of the work is presented in Section 6.

2. PROPOSED LVC AND LVGCC CONTROL STRATEGIES

A simplified model for DGI with voltage control in the standalone as well as current control in grid-connected mode are shown respectively in Figs.2(a,b). The load voltage is the same as grid voltage and DGI works as a current source in the grid connected mode. When the grid is distorted and faulty, DGI changes to standalone mode and acts as a current source. In droop control, as shown in Figs.2(c,d), DGI works like a controlled voltage source by which it is possible to exchange power with the grid and feed the load in standalone mode by controlling the angle and amplitude of the voltage. In terms of hardware, to control the load voltage quality in the grid connected mode, the load has to be separated from the grid by impedance and then it can be controlled. The inductor is the most convenient choice for this purpose because it does not consume any active power. The equivalent proposed DGI circuit in this study is presented in Fig. 3 for which its main aim is feeding load with standard voltage. The existing challenges for the proposed DGI are:

- Selection of a suitable voltage reference for load.
- Presenting internal controllers for tracking voltage reference

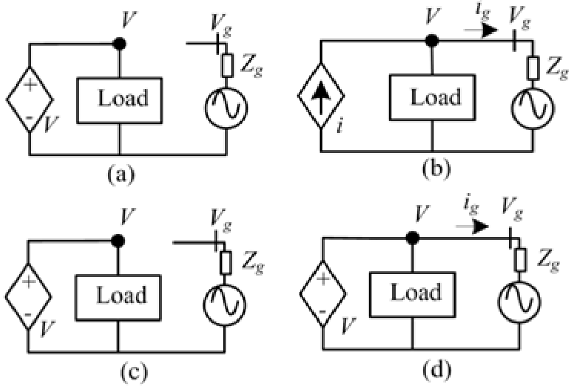

Fig. 2. Equivalent circuit modals of common DGIs. (a) Current control in grid-connected mode. (b) Voltage control in standalone mode. (c) Droop control in grid-connected mode. (d) Droop control in standalone mode.

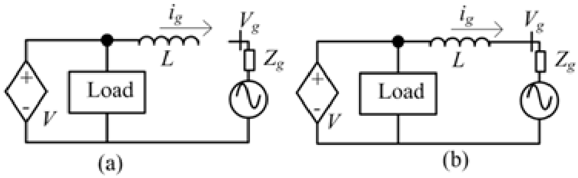

Fig. 3. Equivalent circuit modals of proposed DGI. (a) grid-connected mode. (b) Standalone mode.

- Selection of hardware parameters

The main issue in the proposed control strategies is the selection of load voltage waveform (V), which should be made by the DGI in standalone and grid connected modes. In standalone mode, the load voltage reference is a pure sinusoidal voltage. In the grid connected mode, two different strategies can be carried out depending on the quality of load voltage:

- LVC control strategy: load is fed with high quality voltage, and grid current quality is not considered.
- LVGCC control strategy: load voltage quality and grid current quality are controlled simultaneously.

To explore the difference between these two strategies, assume that the grid has odd harmonics 5, 7, 11, 13, … according to:

$$\begin{aligned} V_g(t) &= V_1 \sin(\omega t) + V_5 \sin(5\omega t + \varphi_5) \\ &+ V_7 \sin(7\omega t + \varphi_7) + ... \end{aligned} \quad (1)$$

The amplitude of the h^{th} harmonic of grid current in grid connected mode is equal to:

$$I_{gh} = \frac{V_h - V_{gh}}{jh2\pi f L} \quad (2)$$

Table 2. DGI capabilities

	LVC	LVGCC	[7-10	[13]	[14-15]	[16-21]	[22-23]	[24]
Controlling of exchanged active power with the grid	√	√	√	√	√	√	√	√
Controlling of exchanged reactive power with the grid			√	√	√	√	√	√
Controlling of grid current		√	√		√	√	√	√
Controlling of inverter power			√		√	√	√	√
Controlling of inverter current			√		√	√	√	√
Controlling load voltage in grid-connected mode	√	√						
Controlling load voltage in standalone mode	√	√		√	√	√	√	
Compensation of load current harmonics	√	√		√			√	√
Seamless Transform	√	√		√	√	√	√	

The load voltage in LVC control strategy will be:

$$LVC : V(t) = V_{1n}\sin(\omega t+\delta),\ \delta \propto P^{*} \quad \textbf{(3)}$$

Where, the load voltage (δ) is calculated based on the active power reference exchanged with grid. In LVC, the current will be sinusoidal due to the fact that load voltage is completely sinusoidal and the h^{th} harmonic amplitude of grid current is equal to:

$$I_{gh} = \frac{-V_{gh}}{jh2\pi fL} \quad \textbf{(4)}$$

In LVGCC control strategy, the addition of a permissible level of grid voltage harmonics to load voltage, reduces harmonics of grid current. The load voltage reference of LVGCC strategy is:

$$\begin{aligned} LVGCC : V(t) &= V_{1n}\sin(\omega t+\delta) + V_{5n}\sin(5\omega t+\varphi_5) \\ &+ V_{7n}\sin(7\omega t+\varphi_7) + ... \end{aligned} \quad \textbf{(5)}$$

The load voltage harmonics are precisely in phase with the grid voltage harmonics in the above equation, but, their amplitudes are equal to the amount given in IEEE 1547 standard (Table.1). The first priority of LVGCC strategy is to feed the load with standard voltage and to benefit from load voltage standard harmonics to remove current harmonics:

$$\begin{cases} Hf_h = \frac{V_h}{V_1} \leq Hf(\max) \\ THD_v \leq THD_{\max} \\ I_h = \frac{V_h - V_{gh}}{jh2\pi fL} \cong 0 \end{cases} \quad \textbf{(6)}$$

As illustrated in Fig. 3, the proposed DGI should connect to the load similar to a voltage source, so a filter with higher order than 2 should be placed between the VSI and load. By placing the second order LC filter between VSI and load a structure with the name DGI with a LC-L filter is created (Fig.4).

In the following section, the implementation of proposed control strategies and hardware design for this DGI will be thoroughly discussed.

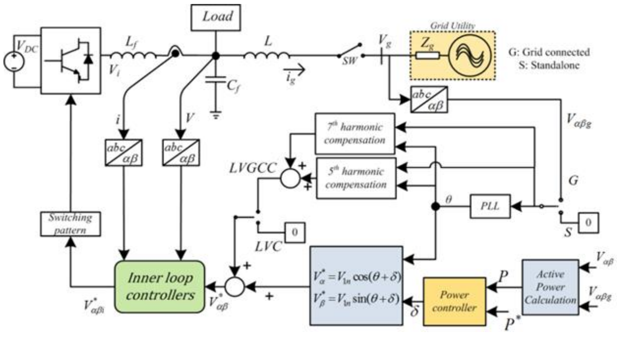

Fig. 4. Proposed DGI with LC-L filter: circuit diagram and implementation of proposed control strategies.

3. IMPLEMENTATION OF PROPOSED CONTROL STRATEGIES

The block diagram of implementation of the proposed control strategies for DGI with LC-L filter is shown in Fig.4, in which a cascade power-voltage-current control method is used. In the proposed control strategies, control of load voltage, grid current control and control of active power exchanged with grid are the objectives. The exchange of reactive power with the grid is out of control.

A. Control loops

Load voltage and grid voltage are used to calculate the power exchange with the grid in the power loop (see Fig.4). The difference between reference power and calculated power is passed through an integral controller. The output of controller is equal to the load voltage phase (δ). Then the voltage reference in grid fundamental frequency is built based on PLL output and the load voltage phase (δ):

$$\begin{cases} \delta = m\int (P^{*} - P)dt \\ V^{*}_{\alpha 1} = V_{1n}\cos(\theta+\delta) \\ V^{*}_{\beta 1} = V_{1n}\sin(\theta+\delta) \end{cases} \quad \textbf{(7)}$$

In the next step, according to the control strategy, the voltage reference is built based on grid voltage harmonics and volt-

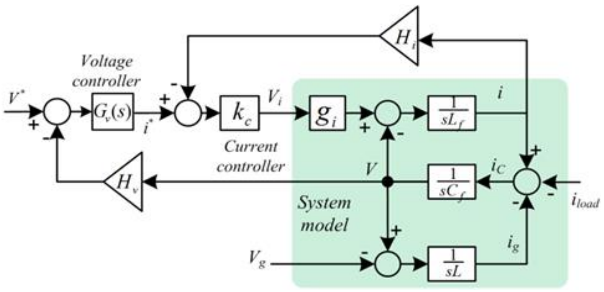

Fig. 5. Inner loops for tracking of voltage reference in proposed DGI with LC-L filter in the stationary reference frame.

age reference in fundamental frequency. The control scheme consisting of inner current loop and outer voltage loop is proposed to track load voltage reference. The block diagram of DGI controller with LC-L filter and proposed controllers are demonstrated in Fig. 5. For designing controllers, separation of current loop and voltage loop is one of the most desirable methods.

In both grid connected and standalone modes, in the stationary reference frame (α axis and β axis), the proposed DGI can be expressed as:

$$\begin{cases} \frac{di}{dt} = \frac{v_i - v}{L_f} - r_f \frac{i}{L_f} \\ \frac{dv}{dt} = \frac{i - i_g - i_{load}}{C_f} \\ \frac{di_g}{dt} = \frac{v - v_g}{L} - r\frac{i}{L} \end{cases} \tag{8}$$

By using a proportional controller in the current loop (Gi(s)=kc), its closed loop function is given as:

$$\frac{i(s)}{i^*(s)} = \frac{g_i H_i k_c (s^2 C_f L + 1)}{s^3 L_f C_f L + s^2 g_i H_i C_f L k_c + s(L_f + L) + g_i H_i k_c} \tag{9}$$

As it can be seen from the above relations, the current loop is a three order system with one real and two complex poles. For designing the voltage loop controller, the conversion function V/i^* is equal to:

$$\frac{V(s)}{i^*(s)} = \frac{s g_i k_c L}{s^3 L_f C_f L + s^2 g_i H_i C_f L k_c + s(L_f + L) + g_i H_i k_c} \tag{10}$$

The relations of the DGI with LC-L filter in Fig. 5 equal to:

$$\begin{cases} V(s) = T_v(s) V^*(s) - Z_o(s) i_{load}(s) - T_{vg}(s) V_g(s) \\ i_g(s) = Y_v V^*(s) - T_i(s) i_{load}(s) - Y_{vg}(s) V_g(s) \end{cases} \tag{11}$$

The transfer functions which are used in the above relations are:

$$\begin{cases} T_v(s) = \frac{V(s)}{V^*(s)} = \frac{s g_i k_c L G_v(s)}{\Delta(s)} \\ Z_o(s) = \frac{V(s)}{i_{load}(s)} = \frac{s^2 L L_f + s g_i k_c L H_i}{\Delta(s)} \\ T_{vg}(s) = \frac{V(s)}{V_g(s)} = \frac{s L_f + s g_i k_c H_i}{\Delta(s)} \\ Y_v = \frac{i_g(s)}{V^*(s)} = \frac{g_i k_c G_v(s)}{\Delta(s)} \\ T_i(s) = \frac{i_g(s)}{i_{load}(s)} = \frac{s L_f + g_i k_c H_i}{\Delta(s)} \\ Y_{vg}(s) = \frac{i_g(s)}{V_g(s)} = \frac{s^2 L_f C_f + s g_i k_c C_f H_i}{\Delta(s)} \end{cases} \tag{12}$$

In the above relations, the system characteristic equation is:

$$\begin{aligned} \Delta(s) &= s^3 L_f C_f L + s^2 g_i H_i C_f L k_c \\ &+ s(L_f + L + L k_c g_i H_v G_v(s)) + g_i H_i k_c \end{aligned} \tag{13}$$

According to the proposed control strategies, the voltage controller has to be able to track a voltage reference consisting of the fundamental frequency and its odd-harmonic frequencies, while, disturbances due to load current and grid voltage makes it difficult to follow the voltage reference. A new voltage controller with the following transfer function is proposed in the voltage loop:

$$G_v(s) = \left(k_{p1} + {}^{k_{i1}}\!/_{s}\right)\left(\frac{\pi^2}{4} - \frac{\pi\omega_e}{2s}\tanh\left(\frac{\pi s}{2\omega_e}\right)\right) \tag{14}$$

The proposed voltage controller is implemented with the least amount of calculations in the stationary reference frame which has an appropriate performance in tracking harmonics. Derivation of a voltage Controller form synchronous reference frame proportional–integral multi-loop controller, its parameters design and evaluation was published in [25]. The controlling parameters of the proposed voltage controller are chosen based on the bandwidth, phase margin and odd harmonic gains in response to the open loop system response.

B. Grid Synchronization

A simple islanding detection based on IEEE 1547 is used to determine DGI operation mode, where according to Fig.6 grid amplitude (Vg) and frequency (f) continuously are checked inside of this flowchart. In the case of a grid outage, a sinusoidal voltage reference with a base frequency is used as a reference. Whenever the grid returns to its normal condition, DGI has to switch to grid connected mode by going through the synchronism procedure.

4. HARDWARE DESIGN

The LC filter has to be used to eliminate switching harmonics, which includes an inductor and a capacitor (see Fig.4). To calculate the size of the inductor and the filter capacitor, firstly the filter cutoff frequency fr is chosen between 10 times of base frequency f and half of switching frequency fs. Then, the inductor is selected according to the maximum allowed ripple of current (Δi) as follows [26]:

$$L_f = \frac{V_{dc}}{3.\Delta i. f_s} m(1-m) \tag{15}$$

Where, m is modulation index of the inverter. Then, capacitor size is calculated according to the following equation:

$$\mathrm{C_f} = \frac{1}{\mathrm{L}_f !_\mathrm{r}^2} \tag{16}$$

Finally, harmonics of grid current can be restricted by choosing grid side inductor L correctly, as follows:

$$\begin{aligned} &\frac{V_{gh}\max}{2h\pi f} < L < \frac{3V^2}{2\pi f P_n}\sin(\delta_{\max}), \\ &h = 5 \qquad\qquad for\ LVC, \\ &h = 11 \qquad\qquad for\, LVGCC, \end{aligned} \tag{17}$$

Where $\delta_{\max}$ is the maximum angle difference between load voltage and grid, which is usually less than 40o. Also,P_n and

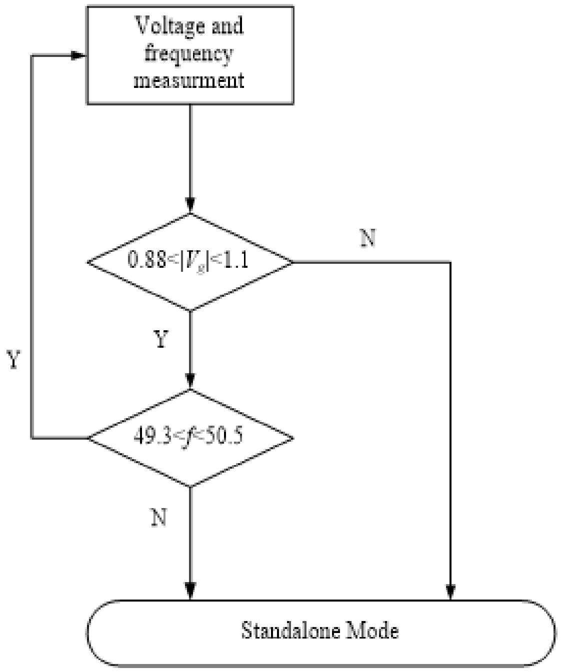

Fig. 6. Islanding detection method based IEEE 1547.

V_{gh} max are the nominal power exchange with the grid and maximum content of grid voltage at harmonic h, respectively. In LVC strategy, L can be enlarged enough to limit current harmonics, but, this leads to the limitation of active power exchange with the grid. In LVGCC strategy, the idea of adding suitable harmonic voltages to load voltage reference are proposed for the restriction of current harmonic amplitudes 5 and 7.

5. DESIGN, SIMULATION AND EVALUATION

To prove the efficiency of the proposed control strategies, a DGI with a LC-L filter with parameters given in Table 3 is simulated, assuming that grid voltage has 5% of 5th harmonic and 4% of 7th harmonic. On the other hand, local load of DGI includes a nonlinear load of 10kW and a linear load of 4kW at 0.8 power factor of 0.8 lagging. To make a proper assessment of conventional DGIs reviewed in the introduction, the DGI with LCL filter and current control scheme introduced in [10] will also be simulated. The parameters of a DGI with LCL filter are completely similar to the data presented in Table.will also be simulated. The parameters of a DGI with LCL filter are completely similar to the data presented in Table. 3. The inveter is simaluted as a 2level voltage source converter in switching mode with 10kHz switching frequency.

A. Frequency domain analysis

Based on the discussion in the previous section and [25] kc=2.5 is selected in the current loop. The proportional factor of the proposed voltage controller (kp1) in the voltage loop is chosen according to bandwidth and phase margin of open loop response. Afterwards, the integral factor is set based on the proportional factor and nominal system parameters (ki1=kp1/RC). For kp1=0.0938 and ki1=234.4, the open loop response of the system is shown in Fig. 7(a). In which the phase margin is 180 degrees and the gain in odd harmonics is more than 40 db, which assures that there is less than 1% steady state error. Fig.7(b) is the system closed loop response. In which the amplitude and response phase in all odd harmonics are about 1∠0°, which indicate that the system is effective in tracking odd harmonics.

Table 3. DGI with LC-L and LCL filters parameters

Description	Symbol	Value
Filter inductance	$L_f + rl$	2.87 mH + 0.05 Ω
Filter capacitor	C_f	$60\mu F$
Interface inductance	L	2 mH + 0.3 Ω
Switching frequency	f_s	10 kHz
Grid voltage	$V_{abc,g}$	380 V
Grid Frequency	f	50 Hz
Inverter DC voltage	$V_D C$	700 V

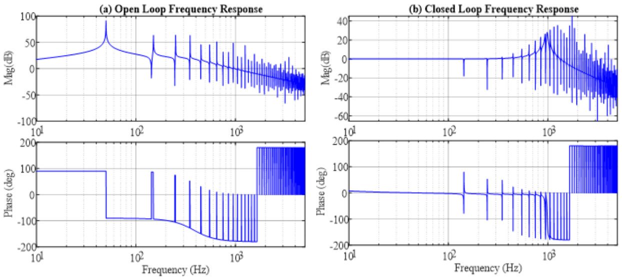

Fig. 7. The frequency response for proposed control scheme: (a) open loop response, (b) closed loop response.

B. Time domain analysis

B.1. Verify the performance of voltage controller

As pointed out in the control loops design section, the voltage controller must be able to track the sinusoidal and nonsinusoidal voltage references under supplying nonlinear load. Proposed voltage controller and proportional resonant controller are among the most efficient controllers for this work. In this section, the performance of two controllers will be compared. The proportional-resonant controller can be formalized as follows [7], [27]:

$$PR = k_p + \sum_{i=1,3,7,11,13,17} \frac{sk_i}{s^2 + 2\omega_{ci}s + i^2\omega^2} \quad (18)$$

Where, $\omega = 2\pi f$ and also ω_{ci}, k_c and k_i are the cutoff frequency, bandwidth frequency, proportional coefficient and resonant controller coefficient, respectively. Simulation of nonsinusoidal voltage reference tracking for LVGCC control strategy with the proposed controller and PR controller are shown in Fig. 8 and and Fig. 9. It can be seen that both controllers are able to track the reference but the proposed controller has a lower computational burden.

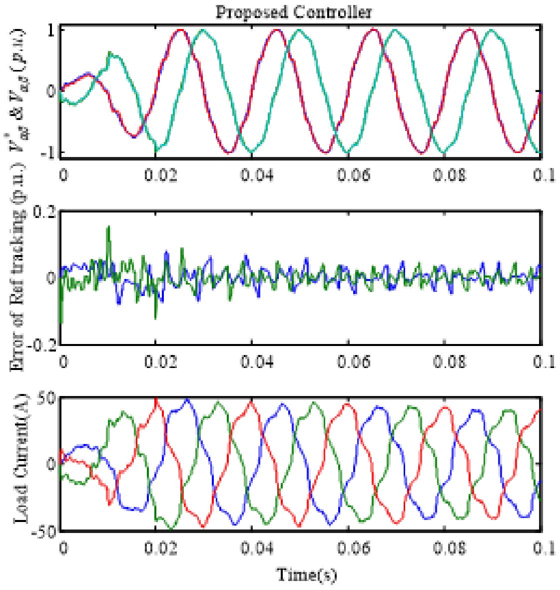

Fig. 8. Performance of proposed voltage controller for tracking of non-sinusoidal voltage reference. From top: load voltage and voltage reference in the stationary reference frame, error of voltage tracking, load current.

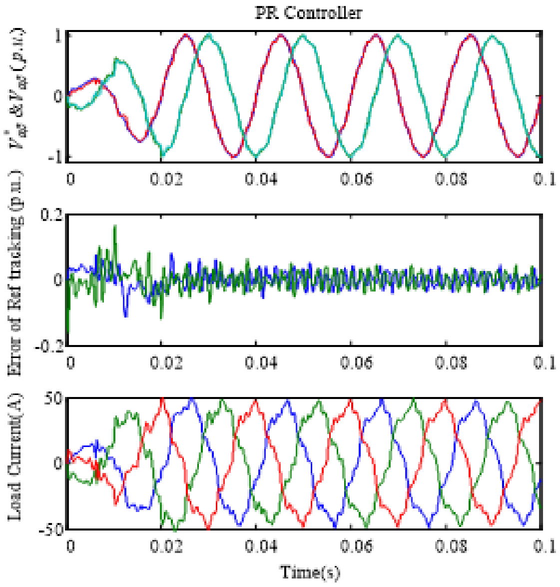

Fig. 9. Performance of PR controller for tracking of non-sinusoidal voltage reference. From top: load voltage and voltage reference in the stationary reference frame, error of voltage tracking, load current.

B.2. Startup process of proposed DGI

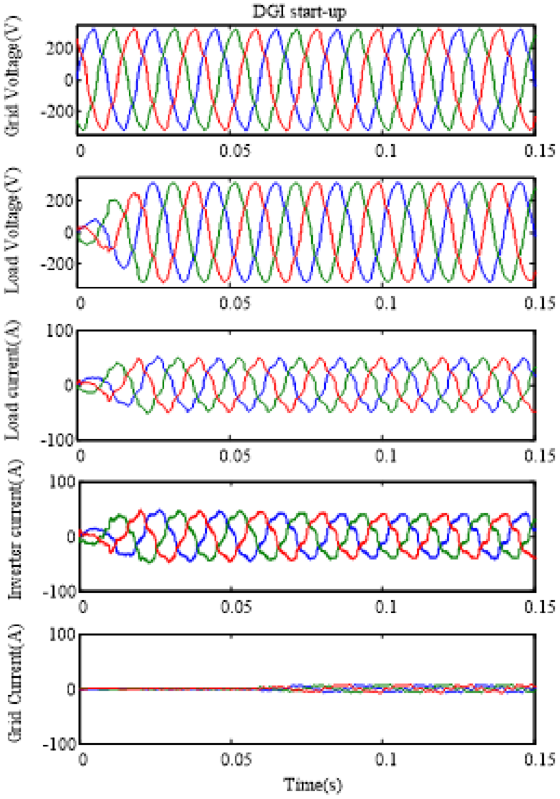

Fig. 10. DGI start-up (switching between operation modes). From down: grid current, inverter current, load current, load voltage, grid voltage.

This part presents the startup process of DGI with an LC-L filter. First, DGI starts in standalone mode and tries to match load voltage and grid voltage in terms of amplitude and phase through control loops. Once the difference between load voltage and grid voltage drops to a certain amount, the circuit breaker will connect the DGI to the grid. The simulation results of star-up is shown in Fig. 10, in which load is fed with standard voltage as well as the inverter current and grid current are under control during connection instance. There is no over current or load voltage distortion during the simulation.

B.3. Change of power reference

In this part of paper, the ability of the proposed control scheme in exchanging the active power with the grid will be analyzed. Controlling of reactive power is out of scope of the control scheme because DGI works as a PV bus. In PV bus, the active power P and the voltage magnitude $|V|$ are specified. Fig. 11 shows the results of a simulation in which the active reference power changes from 0 to 30kW at t=0.15s, then it changes from 30kW to -30kW at t=0.45s. From the obtained results, it can be seen that power reference is tracked with a good transient response. Moreover, the grid current and load voltage waveforms are regulated by the control scheme. In fact, the amount of exchanged power with the grid has not a significant effect on the quality of load voltage, and the load is fed with a completely standard voltage.

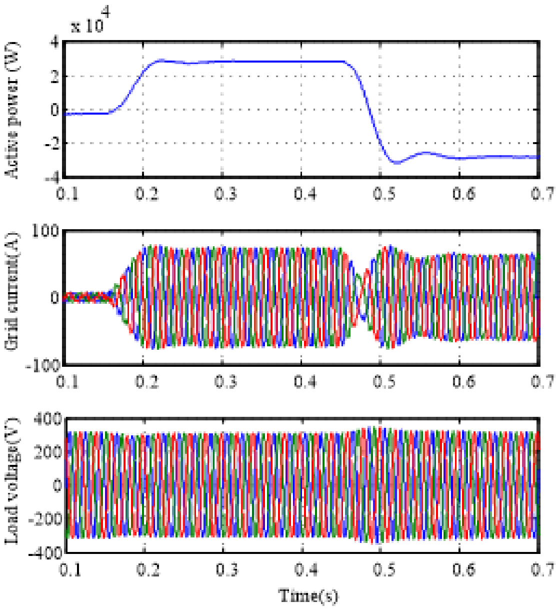

Fig. 11. Simulation results of power reference step change. From top: exchanged power with the grid, grid current, and load voltage.

B.4. Grid Voltage fault

In case of grid voltage faults, DGI has to disconnect from grid and supply local load with standard voltage. In this section, the operation of DGI will be discussed in case of occurrence voltage sag in the grid. The results of 80% voltage sag in the grid voltage at t=0.35 is shown in Fig. 12. It can be seen from Fig. 12 that despite the grid voltage sag, DGI disconnects from the grid and the load is being fed with a standard voltage.

B.5. Comparison with typical control scheme

The comparative study between proposed control and typical control scheme will be driven in this section. In standalone mode, all control schemes work with the same role and they supply the load with pure sinusoidal voltage. Therefore, the comparison should be done in the grid-connected mode where DGI and non-linear load connect to the grid, and DGI has to exchange power to the distorted grid. In this section, the quality of load voltage and quality of grid current will be explored for the evaluation of control schemes. The simulation results of DGI with the LCL filter and current control (CC) scheme according to [10] in the grid connected mode are shown in Fig. 13(a). In CC scheme, the objective is to draw a sinusoidal current with unity power factor from the inverter. However, in this hardware configuration as shown in Fig. 1 if the inverter current is sinusoidal and the load current is non-sinusoidal, then the grid current will be non-sinusoidal with a no unity power factor. The simulation results of the proposed LVGCC and LVC strategies for DGI with LC-L filter in steady state are illustrated in Fig. 13 (b,c). The main purpose of proposed strategies is supplying load with standard voltage independent of grid voltage quality. The results of LVC strategy simulation are presented in Fig. 13(b). It is clear that in spite of the distortion of grid voltage (THD about 6.47%) and nonlinearity of load (THD 11.12%), the load is fed with a standard sinusoidal voltage of THD=1.66%. It can be seen from LVGCC in Fig. 13(c) that adding 5th and 7th harmonics to load voltage leads to improve the grid current quality. It should be pointed out that the improvement of grid current quality, has the consequence of quality reduction of load voltage. In Fig. 14, comparison between Fourier spectrum of load voltage and grid current for control schemes are shown. It can be seen that, in CC scheme although the inverter current is sinusoidal with a THD lower than 1.97%, the grid current is non-sinusoidal with a THD of 7.84% and load is supplied with nonstandard grid voltage (THD=6.47%). Comparison of Fourier spectrums in LVC and LVGCC show that for LVGCC scheme, load voltage and grid current are in IEEE standard range (Table.1). And LVC scheme is acceptable, which only control quality of load voltage.

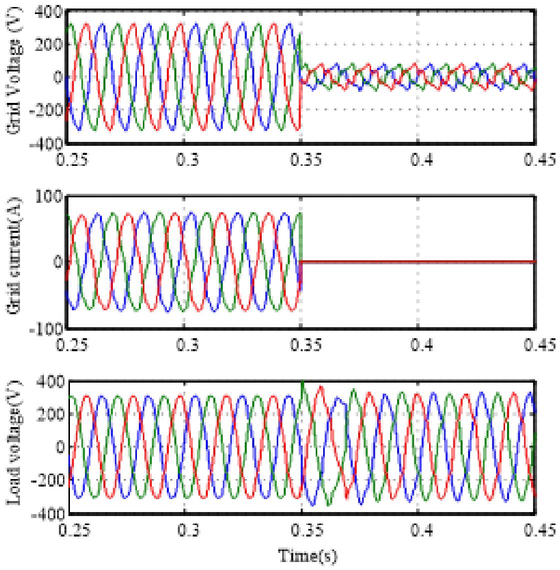

Fig. 12. Simulation results for 80% voltage sag. From down: grid voltage, grid current, load voltage.

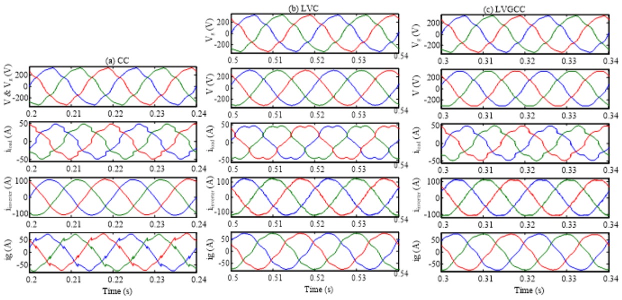

Fig. 13. Simulation results in grid-connected mode: (a) DGI with current control, (b) DGI with LC-L filter and LVC control strategy, (c) DGI with LC-L filter and LVGCC control strategy. From down: grid current, inverter current, load current, load voltage, grid voltage.

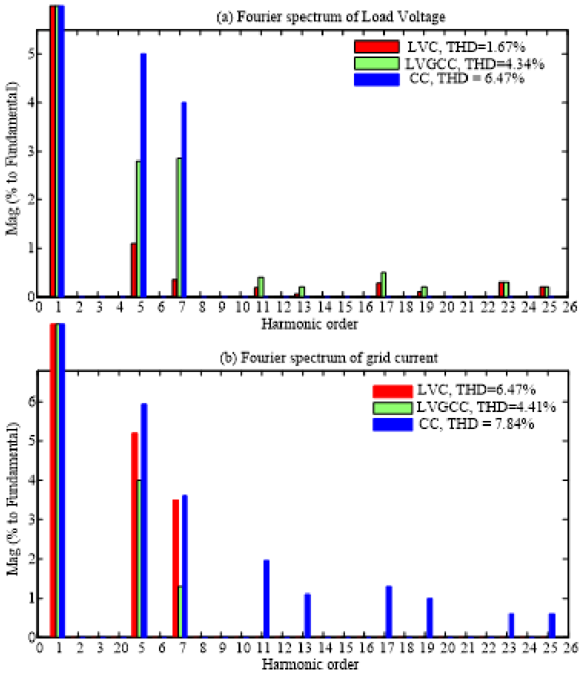

Fig. 14. Fourier spectrum of simulation results in grid-connected mode: (a) Load voltage (b) Grid current.

6. CONCLUSION

This paper proposed two novel control strategies for DGI with LC-L filter in order to supply load with standard voltage in all conditions as well as to compensate nonlinear current harmonics: 1) LVC strategy; feed load with high-quality voltage without any attention to the quality of the current injected to the grid; the fundamental order of current was only controlled in this mode. 2) LVGCC strategy: simultaneous control of load voltage and grid current; in this strategy, it became possible to control harmonics of current injected to the grid by purposely reducing the quality of load voltage. The hardware of DGI and three loops control scheme were designed to achieve load voltage and grid current control capabilities. Comparison of voltage controllers showed that the proposed controller with lower computational burden has non-sinusoidal reference tracking capability, similar to conventional PR controller. Simulation results of the proposed control scheme for operation in standalone mode, grid-connected mode and seamless transfer between modes, verify their performance. Also, comparison with the current control scheme demonstrates that they have more desirable performance in view of load voltage quality as well as the quality of current injected to the grid.

REFERENCES

1. European Commission, “A policy framework for climate and energy in the period from 2020 to 2030,” 2014.
2. E. Salary, M. R. Banaei, and A. Ajami, “Multi-Stage DC-AC Converter Based on New DC-DC Converter for Energy Conversion,” J. Oper. Autom. Power Eng., vol. 4, no. 1, pp. 42–53, 2016.
3. A. Hatefi einaddin, A. Sadeghi Yazdankhah, and R. Kazemzadeh, “Power Management in a Utility Connected Micro-Grid with Multiple Renewable Energy Sources,” J. Oper. Autom. Power Eng., vol. 5, no. 1, pp. 1–10, 2017.
4. H. Moayedirad and M. A. S. Nejad, “Increasing the Efficiency of the Power Electronic Converter for a Proposed Dual Stator Winding Squirrel-Cage Induction Motor Drive Using a Five-Leg Inverter at Low Speeds,” J. Oper. Autom. Power Eng., vol. 6, no. 1, pp. 23–39, 2018.
5. F. Sedaghati, S. Mohammad Salehian, H. Shayeghi, and E. Shokati Asl, “A Configuration of Double Input Z-Source DC-DC Converter for Standalone PV/Battery System Application,” J. Energy Manag. Technol., vol. 2, no. 3, pp. 60–69, Sep. 2018.
6. M. Azizi, A. Fatemi, M. Mohamadian, and A. Y. Varjani, “Integrated solution for microgrid power quality assurance,” IEEE Trans. Energy Convers., vol. 27, no. 4, pp. 992–1001, 2012.
7. M. Hosseinpour and N. Rasekh, “A Single-Phase Grid-tied PV based Trans-Z-Source Inverter Utilizing LCL filter and Grid Side Current Active Damping,” J. Energy Manag. Technol., vol. 0, Mar. 2019.
8. A. R. N. Sefiddashti, G. R. Arab Markadeh, A. Elahi, and R. Pouraghababa, “Low Voltage Ride Through Enhancement Based on Improved Direct Power Control of DFIG under Unbalanced and Harmonically Distorted Grid Voltage,” J. Oper. Autom. Power Eng. Winter Spring, vol. 4, no. 1, pp. 16–28, 2016.
9. F. S. Pai, “An improved utility interface for microturbine generation system with stand-alone operation capabilities,” IEEE Trans. Ind. Electron., vol. 53, no. 5, pp. 1529–1537, 2006.
10. I. J. Balaguer, S. Member, Q. Lei, S. Yang, U. Supatti, and S. Member, “Control for Grid-Connected and Intentional Islanding Operations of Distributed Power Generation,” vol. 58, no. 1, pp. 147–157, 2011.
11. A. Kulka, T. Undeland, S. Vazquez, and L. G. Franquelo, “Stationary frame voltage harmonic controller for standalone power generation,” in 2007 European Conference on Power Electronics and Applications, EPE, 2007.
12. T.-V. Tran, T.-W. Chun, H.-H. Lee, H.-G. Kim, and E.-C. Nho, “PLL-Based Seamless Transfer Control Between Grid-Connected and Islanding Modes in Grid-Connected Inverters,” IEEE Trans. Power Electron., vol. 29, no. 10, pp. 5218–5228, Oct. 2014.
13. Q.-C. Zhong and T. Hornik, “Cascaded Current–Voltage Control to Improve the Power Quality for a Grid-Connected Inverter With a Local Load,” IEEE Trans. Ind. Electron., vol. 60, no. 4, pp. 1344–1355, Apr. 2013.
14. M. N. Arafat, S. Palle, Y. Sozer, and I. Husain, “Transition Control Strategy Between Standalone and Grid-Connected Operations of Voltage-Source Inverters,” IEEE Trans. Ind. Appl., vol. 48, no. 5, pp. 1516–1525, Sep. 2012.

15. D. S. Ochs, B. Mirafzal, and P. Sotoodeh, “A Method of Seamless Transitions Between Grid-Tied and Stand-Alone Modes of Operation for Utility-Interactive Three-Phase Inverters,” IEEE Trans. Ind. Appl., vol. 50, no. 3, pp. 1934–1941, May 2014.

16. M. Shi, X. Chen, J. Zhou, Y. Chen, J. Wen, and H. He, “Advanced Secondary Voltage Recovery Control for Multiple HESSs in a Droop-controlled DC Microgrids,” IEEE Trans. Smart Grid, vol. 3053, no. c, 2018.

17. J. Zhou and P.-T. Cheng, “A modified droop control for accurate reactive power sharing in distributed generation microgrid,” IEEE Trans. Ind. Appl., pp. 1–1, 2019.

18. X. Meng, J. Liu, and Z. Liu, “A generalized droop control for grid-supporting inverter based on comparison between traditional droop control and virtual synchronous generator control,” IEEE Trans. Power Electron., vol. PP, no. c, p. 1, 2018.

19. D. Yang, X. Ruan, and H. Wu, “Impedance shaping of the grid-connected inverter with LCL filter to improve its adaptability to the weak grid condition,” IEEE Trans. Power Electron., vol. 29, no. 11, pp. 5795–5805, 2014.

20. B. Wei, A. Marzabal, R. Ruiz, J. M. Guerrero Ge, and J. Vasquez, “DAVIC: A New Distributed Adaptive Virtual Impedance Control for Parallel-Connected Voltage Source Inverters in Modular UPS System,” IEEE Trans. Power Electron., vol. 8993, no. c, 2018.

21. A. Tarrasó, J. I. Candela, J. Rocabert, and P. Rodriguez, “Grid voltage harmonic damping method for SPC based power converters with multiple virtual admittance control,” in 2017 IEEE Energy Conversion Congress and Exposition, ECCE 2017, 2017, vol. 2017–Janua, pp. 64–68.

22. R. Ghanizadeh, M. Ebadian, and G. B. Gharehpetian, “Control of Inverter-Interfaced Distributed Generation Units for Voltage and Current Harmonics Compensation in Grid-Connected Microgrids,” J. Oper. Autom. Power Eng., vol. 4, no. 1, pp. 66–82, 2016.

23. morteza afrasiabi and E. Rokrok, “A hierarchical control scheme for compensating voltage distortions in an inverter based microgrid,” J. Energy Manag. Technol., vol. 1, no. 3, pp. 52–59, Dec. 2017.

24. “An optimized direct control method applied to multilevel inverter for microgrid power quality enhancement,” Int. J. Electr. Power Energy Syst., vol. 107, pp. 496–506, May 2019.

25. M. Shahparasti, M. Mohamadian, A. Yazdian, and M. Amini, “Derivation of a Stationary-Frame Single Loop Controller for Three Phase Standalone Inverter Supplying Nonlinear Loads,” vol. 29, no. 9, pp. 5063–5071, 2013.

26. Y. Tang, P. C. Loh, P. Wang, F. H. Choo, and F. Gao, “Exploring inherent damping characteristic of LCL-filters for three-phase grid-connected voltage source inverters,” IEEE Trans. Power Electron., vol. 27, no. 3, pp. 1433–1443, 2012.

27. J. Fallah Ardashir, A. Mohammadpour Shotorbani, H. khoun-Jahan, and M. Sabahi, “Fractional PR Control of a Grid Tied Flying Capacitor Inverter for PV Applications,” J. Energy Manag. Technol., vol. 3, no. 2, pp. 58–64, Jun. 2019.